Cell Reports
Report

Constitutional Chromothripsis Rearrangements Involve Clustered Double-Stranded DNA Breaks and Nonhomologous Repair Mechanisms

Wigard P. Kloosterman,[1,*] Masoumeh Tavakoli-Yaraki,[1] Markus J. van Roosmalen,[1] Ellen van Binsbergen,[1] Ivo Renkens,[1] Karen Duran,[1] Lucia Ballarati,[2] Sarah Vergult,[3] Daniela Giardino,[2] Kerstin Hansson,[4] Claudia A.L. Ruivenkamp,[4] Myrthe Jager,[1] Arie van Haeringen,[4] Elly F. Ippel,[1] Thomas Haaf,[5] Eberhard Passarge,[6] Ron Hochstenbach,[1] Björn Menten,[3] Lidia Larizza,[2,7] Victor Guryev,[8] Martin Poot,[1] and Edwin Cuppen[1,8,*]

[1]Department of Medical Genetics, University Medical Center Utrecht, Universiteitsweg 100, 3584 CG Utrecht, The Netherlands
[2]Laboratorio di Citogenetica Medica e Genetica Molecolare, Centro di Ricerche e Tecnologie Biomediche, IRCCS-Istituto Auxologico Italiano, Via Ariosto 13, 20145 Milano, Italy
[3]Center for Medical Genetics, Ghent University Hospital, De Pintelaan 185, B-9000 Ghent, Belgium
[4]Leiden University Medical Center, Department of Clinical Genetics, Albinusdreef 2, 2333 ZA Leiden, The Netherlands
[5]Institute of Human Genetics, Würzburg University, 97074 Würzburg, Germany
[6]Institut für Humangenetik, Universitätsklinikum Essen, Hufelandstr. 55, D-45122 Essen, Germany
[7]University of Milan, San Paolo School of Medicine, Via A. di Rudinì 8, 20142, Milano, Italy
[8]Hubrecht Institute and University Medical Center Utrecht, Uppsalalaan 8, 3584 CT Utrecht, The Netherlands
*Correspondence: w.kloosterman@umcutrecht.nl (W.P.K.), e.cuppen@hubrecht.eu (E.C.)
DOI 10.1016/j.celrep.2012.05.009

SUMMARY

Chromothripsis represents a novel phenomenon in the structural variation landscape of cancer genomes. Here, we analyze the genomes of ten patients with congenital disease who were preselected to carry complex chromosomal rearrangements with more than two breakpoints. The rearrangements displayed unanticipated complexity resembling chromothripsis. We find that eight of them contain hallmarks of multiple clustered double-stranded DNA breaks (DSBs) on one or more chromosomes. In addition, nucleotide resolution analysis of 98 breakpoint junctions indicates that break repair involves nonhomologous or microhomology-mediated end joining. We observed that these eight rearrangements are balanced or contain sporadic deletions ranging in size between a few hundred base pairs and several megabases. The two remaining complex rearrangements did not display signs of DSBs and contain duplications, indicative of rearrangement processes involving template switching. Our work provides detailed insight into the characteristics of chromothripsis and supports a role for clustered DSBs driving some constitutional chromothripsis rearrangements.

INTRODUCTION

Recently, a new genome rearrangement phenomenon has emerged from the study of highly complex rearrangements in cancer genomes involving frequent oscillations between only two copy number states (Stephens et al., 2011). This phenomenon has been termed chromothripsis and may have resulted from localized shattering of one or several chromosomes and subsequent assembly of resulting chromosomal pieces by nonhomologous end joining (NHEJ). Further studies have identified several instances of somatic chromothripsis rearrangements in a wide variety of cancer specimens (Magrangeas et al., 2011; Kloosterman et al., 2011b; Molenaar et al., 2012; Rausch et al., 2012; Maher and Wilson, 2012). We and others have shown that de novo complex balanced translocations in patients with developmental defects arose from a similar chromosome shattering mechanism (Kloosterman et al., 2011a; Chiang et al., 2012).

A replication-based model (MMBIR, microhomology-mediated break-induced replication) has been proposed for complex rearrangements in the germline that involve copy losses and gains and contain microhomologous sequences at breakpoint junctions (Hastings et al., 2009a, 2009b). Recently, complex genomic rearrangements involving multiple and region-focused copy number changes on one chromosome, were also ascribed to MMBIR and it was speculated that MMBIR could be an explanation for chromothripsis in cancer cells (Liu et al., 2011). In support of this, Crasta et al. proposed that chromosome pulverization could occur due to defects in DNA replication and repair in micronuclei resulting from errors in mitosis (Crasta et al., 2012).

Given the considerable controversy regarding the mechanisms driving complex rearrangements in cancer and development disorders, we here investigated the genetic architecture of ten constitutional complex chromosomal rearrangements (CCRs) using genome-wide long mate-pair sequencing, copy number profiling, and breakpoint-junction sequencing. We found that in eight cases the rearrangements are characterized by multiple clustered double-stranded DNA breaks (DSBs) and break repair was driven by end-joining mechanisms. These

findings suggest that these rearrangements involve chromosome shattering similarly as originally proposed for chromothripsis in cancer (Stephens et al., 2011). The other two rearrangements display distinct molecular characteristics. They do not show signs of DSBs and contain complex copy number changes including copy gains, resembling the chromothripsis-like chromosome catastrophes caused by template switching (Hastings et al., 2009a; Liu et al., 2011). Our findings suggest that chromosome shattering by DSBs results in a distinct type of chromothripsis rearrangements and exists next to processes involving template switching.

RESULTS

Genomic Analysis of Ten Constitutional CCRs

To gain insight in the characteristics of complex constitutional rearrangements, we here analyzed all breakpoints of ten constitutional CCRs by mate-pair sequencing, array analysis, and fusion-point sequencing (Tables S1, S2, and S3; Extended Experimental Procedures). The CCRs were solely selected based on prior evidence indicating more than two breakpoints (de Pater et al., 2002; Giardino et al., 2006; Ballarati et al., 2009; Poot et al., 2009) (Table S1). Hundreds of CCRs with similar karyotypes as the ones selected here have been described in literature (Astbury et al., 2004; Borg et al., 2005; Gribble et al., 2005; De Gregori et al., 2007; Pellestor et al., 2011). Eight of the CCRs had occurred de novo and two CCRs were transmitted from a mother to her child (Table S1). Based on mate-pair sequencing, we identified between 3 and 24 inter- and intrachromosomal breakpoint junctions per CCR. The breakpoint junctions were independently validated by PCR and capillary sequencing. Where possible, parents were included in the validation assays (Table S3). For eight of the CCRs (patients 1–8), plotting the breakpoint junctions onto the reference genome revealed that closely spaced junction points (i.e., the exact genomic coordinates on the reference genome where the junctions occurred) form pairs on the reference genome (Figures 1A and S1). We considered two junction points as a pair when their relative distance was below 1 kb. Furthermore, one junction point in such a pair is connected at its tail (T) side and the other junction point in a pair is connected at its head (H) side. For clarity, we have schematically depicted the concepts of breakpoint junction, orientation, and junction-point pair in Figure 1B. The observation of a junction-point pair is most simply explained by the repair of both free DNA ends resulting from a DSB. We observed that the free DNA ends are repaired by fusion to other (remote) chromosome fragments (which also resulted from DSBs as suggested by the presence of junction-point pairs), leading to complex inter- and intrachromosomal rearrangements. Chromosomal breaks were occurring on one (patients 5 and 8) or several chromosomes (five in patient 7) and showed significantly more clustering along the chromosome than expected by chance ($p < 0.001$, Figure S2). The derivative chromosomes of patient 1 and patient 2 were reconstructed based on the breakpoint junctions identified by the mate-pair sequencing (Figures 1B and 2). The derivative chromosomes were matching the karyotypes as previously established based on cytogenetic analysis (Figure 2A) (Ballarati et al., 2009).

We performed copy number analysis of these eight CCRs to determine whether losses or gains had occurred as a result of the many inter- and intrachromosomal breakpoint junctions (Figures 1A and S1; Table S1). We only observed deletions, but no copy gains. Deletions are flanked by both inter- or intrachromosomal breakpoint junctions (Figure 1, patients 1, 6, and 8). This deletion architecture is different from a "classic deletion," where both flanks of the deletion have been fused to each other. Notably, junction-point pairs were not identified at deletion borders (Figure 1; Figure S1, black arrows). The rearrangement of patient 7 was copy neutral, despite a massive amount of 24 breakpoint junctions. For four de novo CCRs, we tested the parental origin of the rearrangements by SNP-array analysis of deletion intervals in the father, mother, and patient. This demonstrated that these rearrangements had occurred on paternal chromosomes (Table S4). The parents had normal karyotypes and the age of these four fathers ranged between 29 and 41.

Our data suggest that multiple clustered double-stranded DNA breaks triggered the eight CCRs described here. This led to copy balanced rearrangements or rearranged chromosomes with sporadic deletions.

Breakpoint Characteristics of Eight Constitutional Chromothripsis Rearrangements

To further characterize the process of break repair in the eight constitutional chromothripsis CCRs, we analyzed the sequences of 98 breakpoint junctions by PCR-based capillary sequencing (Figure 3A, Figure S3). Most junctions displayed homology of 1–7 nucleotides (45%) or absence of homology (29%). For 26% of junctions, we observed short insertions of 1–97 nontemplated nucleotides. For patient 8, we observed several long nontemplated insertions of up to 97 bp at the breakpoint junctions (Table S3). These inserted fragments did not match with any sequence in the human reference genome and were substantially longer than the nontemplated insertions for the breakpoint junctions in the other patients. In addition, we did observe multiple losses for patient 8 (Table S5), which is in line with prior observations (Simsek and Jasin, 2010).

Based on the capillary sequencing of breakpoint junctions, we could also derive the precise characteristics of 56 junction-point pairs (Table S5; Figure 1B). Junction-point pairs are considered to indicate the occurrence of DSBs. At some positions of DSBs, gains and losses of one or several nucleotides occurred, possibly following repair of staggered cuts or exonuclease digestion of free DNA ends, respectively (Figures 3B and 3C) (Gajecka et al., 2008; Lieber, 2008; Simsek and Jasin, 2010). Together, our data suggest that break repair in the eight chromothripsis CCRs involved canonical or noncanonical NHEJ (explaining the blunt fusions) or MMEJ (explaining the fusions with microhomology) (McVey and Lee, 2008; Lieber, 2010; Simsek and Jasin, 2010). However, we should note that break repair mechanism cannot be precisely inferred from junction sequences alone.

Based on the spacing between adjacent junction points on the reference genome, we could infer the occurrence of deletions of several kilobases in size that were too small to be unequivocally detected by sequence coverage depth analysis or array analysis (see Figure 1B for a schematic example). For

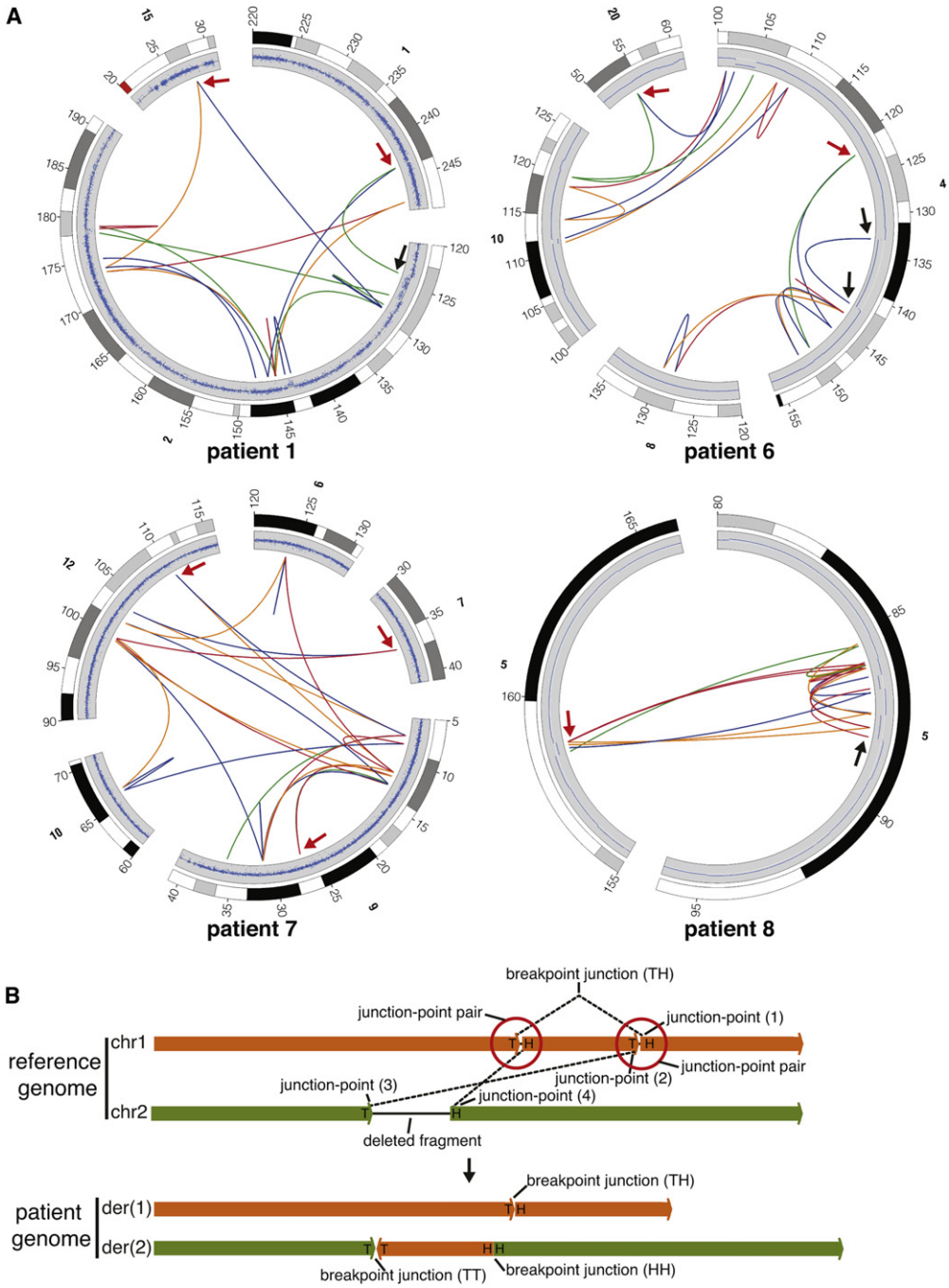

Figure 1. Overview of Breakpoint Junctions Involved in Constitutional CCRs

(A) Visualization of breakpoints junctions of complex rearrangements in patients 1, 6, 7, and 8 using circos plots. The colored lines indicate breakpoint junctions. These are based on the mate-pair data and can be in either of four orientations: HH (head-head), red lines; TT (tail-tail), yellow lines; TH (tail-head), blue lines; HT (head-tail), green lines (low coordinate to high coordinate). The outer circle displays the chromosome ideogram and the inner circle displays the copy number profile based on SNP array data (patient 1 and 7) or depth of coverage analysis (patient 6 and 8). Red arrowheads indicate examples of junction-point pairs and black arrowheads indicate examples of single junction-points flanking deletions.

(B) Schematic drawing indicating the terminology used in this paper. A breakpoint junction can occur in each of four different orientations between intra- or interchromosomal genomic fragments: HH, TT, TH, and HT. The positions on the reference genome (i.e., genomic coordinate) where the breakpoint-junction starts and ends are called junction points. Junction points form a pair if they are in close proximity on the reference genome (with a distance of <1,000 bp). In addition, one junction point in a pair should have its T side connected to another fragment, while the other junction point should have its H side connected to another fragment. Junction point (1) and junction point (2) form a pair. A pair of junction points is the result of a repaired DSB, because a DSB generates two free DNA ends. Each of these ends can be fused to other chromosomal fragments, resulting in a junction-point pair. Break repair may result in erosion of the ends by

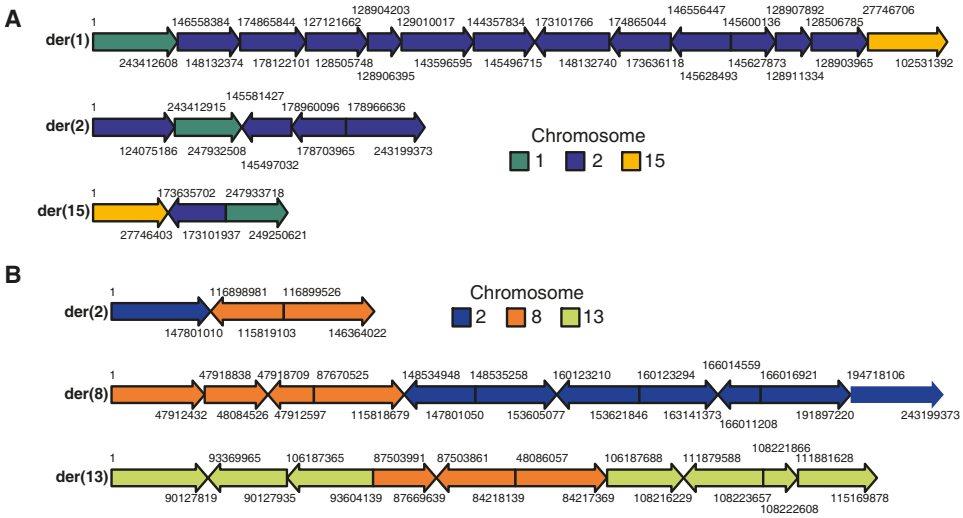

Figure 2. Reconstruction of Derivative Chromosomes for Patients 1 and 2 Based on Mate-Pair Data

(A) Reconstructed derivative chromosomes for patient 1. The derivative chromosomes match the previous FISH and karyotyping analysis of this patient (Ballarati et al., 2009).

(B) Reconstructed derivative chromosomes for patient 2. The reconstructed derivative chromosomes are in line with the karyotype as based on cytogenetic analysis (Table S1). Derivative chromosomes were reconstructed based on the de novo breakpoint junctions that we identified in these patients, similarly as we have demonstrated before (Kloosterman et al., 2011a). The chromosomal coordinates of junction points are based on the mate-pair data as provided in Table S3. Chromosomes are not drawn to scale.

example, in patient 1 we identified adjacent junction points that suggested the occurrence of two deletions of 6,041 and 18,231 bp in size, respectively (Figure 3D). Quantitative (qPCR) analysis showed that these two regions were indeed heterozygously deleted in patient 1, but not in both parents (Figure 3D). For all predicted deletion intervals we calculated normalized sequence coverage depth relative to a common reference sample (Table S5), which confirmed the deletions. Deletions could arise from erosion of the free DNA ends resulting from a DSB or be the result of two adjacent DSBs. Based on our breakpoint data, we could not distinguish between these two possibilities. All together, the dynamic size range of the deletion spectrum (1 bp to 8.8 Mb) associated with DSBs adds another level of complexity to constitutional chromothripsis rearrangements.

Two Complex Rearrangements Involving Replicative Processes

For two of the ten CCRs described here (patients 9 and 10), we observed different breakpoint characteristics as compared to the eight chromothripsis rearrangements described above. One of these cases contained an inherited complex rearrangement on chromosome X and the other involved four de novo duplications on chromosomes 4, 8, and 14 (patients 9 and 10, Table S1). Most notably, we found that the junction points for these two rearrangements do not form pairs on the reference genome (Figure 4). Therefore, we regard it unlikely that a chromosome-shattering event as a result of simultaneous DSBs triggered these two rearrangements. For patient 9, we identified three unique breakpoint junctions that align with the deletion and the two duplications (Figure 4A). For patient 10, we found breakpoint junctions for three of the four de novo duplications. Together with coverage depth analysis, these breakpoint junctions showed that three tandem duplications had occurred in patient 10. For the fourth duplication on chromosome 14, we only found evidence based on depth of coverage analysis using both parents as a reference (Figure 4B). The findings for patients 9 and 10 can be explained by template-switching events during replication, which is in line with the MMBIR mechanism as previously reported (Hastings et al., 2009a; Liu et al., 2011).

DISCUSSION

Here, we provide a comprehensive analysis of the breakpoints of ten constitutional CCRs. We found that eight CCRs exhibited hallmarks of multiple simultaneous double-stranded DNA breaks on one or several chromosomes. The other two complex rearrangements were likely caused by replication errors involving template switching. The two classes of rearrangements that we observed here likely represent distinct instances of chromothripsis rearrangements as has been previously

exonuclease digestion or addition of extra nucleotides. See Figure 3B for a detailed overview of losses and gains at breakpoint regions. Junction point (3) and junction point (4) do not form a pair, because they are not in close physical proximity. The genomic segment in between junction point (3) and junction point (4) is deleted, because it is not connected to other fragments at its H and T sides. H, head; T, tail.

See also Figures S1 and S2 and Tables S1, S2, S3, and S4.

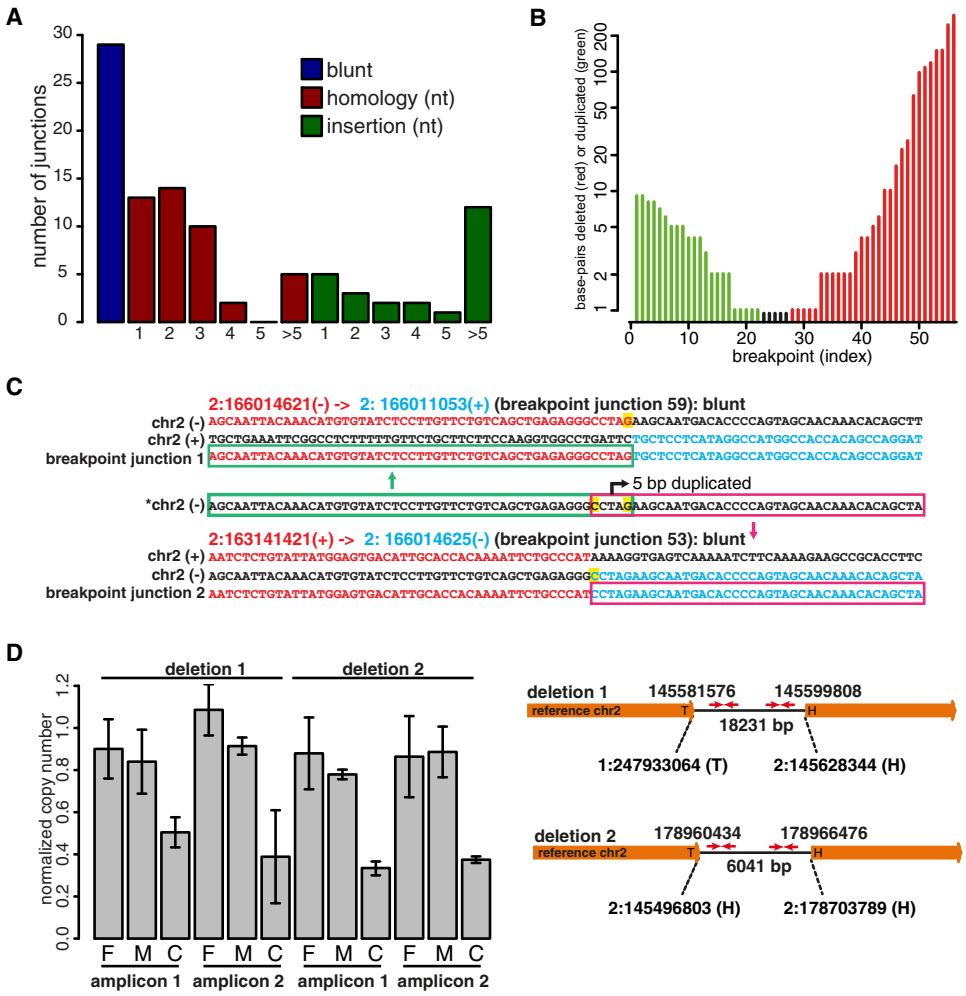

Figure 3. Characteristics of Eight Constitutional Chromothripsis Rearrangements

(A) Bar diagram showing the numbers of bluntly ligated breakpoint junctions (blue bar), breakpoint junctions with one or more nucleotides microhomology (red bars) and breakpoint junctions containing nontemplated insertions (green bars).

(B) Bar diagram showing the loss (red) and gain (red) of nucleotides caused by repair of 56 DSBs. The breakpoint erosion was inferred from capillary sequencing reads across breakpoint junctions. Black bars indicate breaks with no losses or gains.

(C) Sequence composition of two breakpoint junctions that together create a junction-point pair on reference chromosome 2 (patient 2). The breakpoint-junction sequencing reads were aligned to the reference genome. Sequence homology to normal genomic sequences is indicated in light blue and red. The genomic sequence from chromosome 2 marked with an asterisk (*) shares homology with breakpoint junction 1 (green box) and breakpoint junction 2 (pink box). Both stretches of homology overlap in the middle, showing that these 5 bp ended up in both breakpoint-junction sequences and are duplicated. Chromosomal coordinates indicate the junction point for each of the two genomic sequences that form a breakpoint junction. Both coordinates are indicated in the genomic sequence by a yellow box. The red coordinate for breakpoint junction 1 and the blue coordinate for breakpoint junction 2 together form a pair on reference chromosome 2. The breakpoint-junction numbers correspond to the numbering in Table S3.

(D) qPCR analysis of two small de novo deletions (6,041 bp and 18,231 bp) on chr 2 in patient 2 that were predicted based on the mate-pair analysis. The bar diagram displays the relative copy number for the amplified fragments within the deletion intervals in patient 2 and the father and mother. Error bars represent SDs based on $2^{\wedge}(-\Delta\Delta Ct)$ values from triplicate experiments. Red arrows indicate primer pairs. Breakpoint junctions flanking the deleted fragments are indicated by genomic coordinates.

See also Figure S3 and Table S5.

proposed (Chen et al., 2011; Liu et al., 2012; Maher and Wilson, 2012).

By careful analysis of breakpoint junctions, we derived precise molecular characteristics for the eight chromothripsis rearrangements that were caused by multiple DSBs and we conclude that (1) rearrangements can be confined to a single chromosome (patients 5 and 8) or multiple chromosomes (e.g., five in patient 7), (2) rearrangements may lead to sporadic deletions (including small deletions of only a few hundred base pairs), but can also explain copy neutral rearrangements (patient 7), (3) DSBs are clustered, (4) break repair involves nonhomologous or microhomology-mediated repair mechanisms, and (5) rearrangements occur on paternal chromosomes.

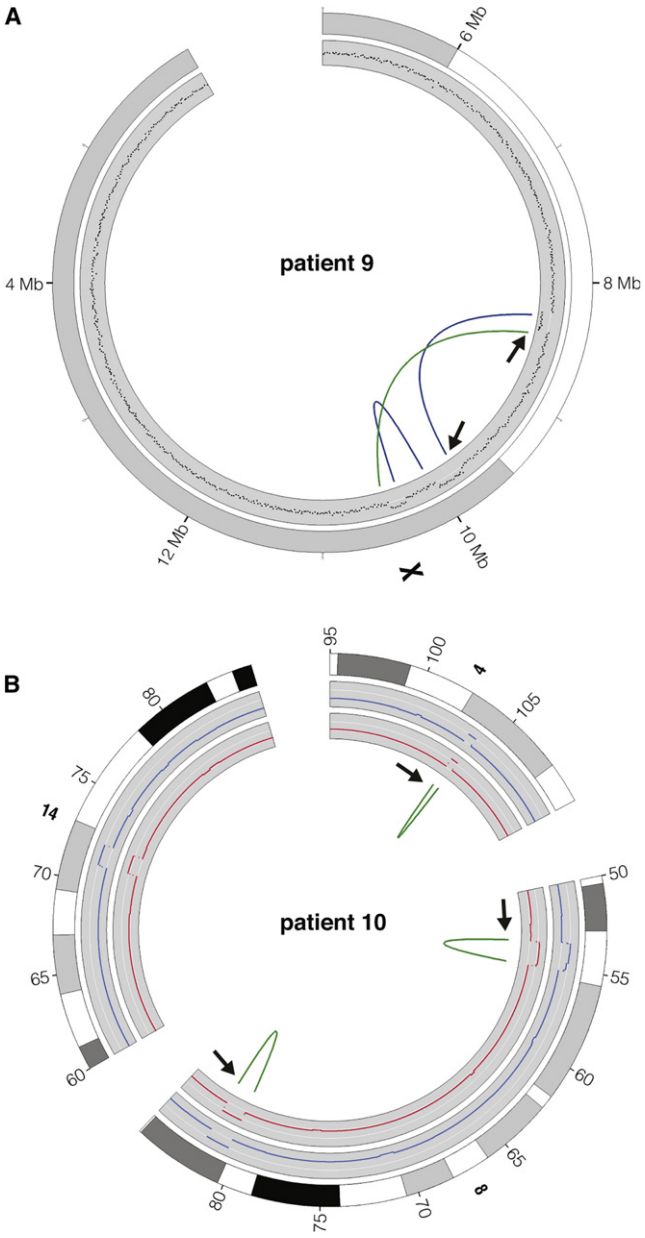

Figure 4. Circos Plot of Mate-Pair and Copy Number Analysis of Two Chromothripsis Rearrangements Involving Duplications and a Deletion

(A) A maternally inherited complex rearrangement in patient 9 involves two duplications and one deletion on chr X. Mate-pair analysis resulted in the identification of three breakpoint junctions, which indicate three template switches. The copy number changes in the inner circle are based on arrayCGH data and can be explained by the three template-switching events.

(B) Circos plot of mate-pair and copy number analysis of a de novo rearrangement involving four duplications on chr 4, 8, and 14 in patient 10. The inner two circles display the copy number profile based on depth of coverage analysis of the patient sequencing data compared to the sequencing data of the father (blue profile, middle circle) and mother (red profile, inner circle). The green colored lines indicate de novo breakpoint junctions. All three breakpoint junctions have a head-to-tail (HT) orientation, which is a signature corresponding to a tandem duplication. We did not identify any other de novo rearrangements on chr 8 in this patient. The three tandem duplications have most likely arisen through three template-switching events during DNA replication. The junction points do not form pairs as for the chromothripsis rearrangements (black arrows).

Several hundred sporadic patients carrying constitutional de novo CCRs have been described over the past years (Astbury et al., 2004; Medvedev et al., 2009; Pellestor et al., 2011). CCRs often display similar karyotypes as for the eight chromothripsis rearrangements identified here (Houge et al., 2003; Borg et al., 2005; Granot-Hershkovitz et al., 2011). In addition, cryptic deletions are frequently coinciding with breakpoints of CCRs, while duplications are hardly found (Gribble et al., 2005; De Gregori et al., 2007; Schluth-Bolard et al., 2009; Feenstra et al., 2011). This suggests that many published rearrangements may have been caused by chromosome shattering and repair, similar as described for the eight chromothripsis CCRs described here. Thus, chromosome shattering and repair may be a common mechanism driving formation of constitutional CCRs and exists next to processes involving template switching (Liu et al., 2011). We cannot draw conclusions about the relative contribution of both processes to the occurrence of constitutional chromothripsis rearrangements. Effects on viability of the fetus will, among others, influence such estimates.

A first hypothesis on a possible mechanism that may cause chromothripsis came from a recent study showing that lagging chromosomes are pulverized as a consequence of replication errors in micronuclei resulting from mitotic errors (Crasta et al., 2012). The chromosome catastrophes described by Liu et al. (2011) indeed point at a replicative mechanism of origin of some constitutional chromothripsis-like rearrangements (Liu et al., 2011). In contrast, we here show eight rearrangements that involve clustered DSBs and nonhomologous repair, resulting in complex derivative chromosomes with sporadic deletions (Figures 1, 2, and 3). It could be that both rearrangement classes represent two different outcomes resulting from a similar molecular trigger, such as described by Crasta et al. (2012). The data from four patients show a paternal origin of the CCRs. This is in line with previous reports that demonstrated a paternal bias for CNV or CCR formation, which is possibly due to the larger number of mitotic divisions during gametogenesis in males compared to females (Gribble et al., 2005; Hehir-Kwa et al., 2011).

In conclusion, by analyzing ten constitutional CCRs by the same analytical methods, we demonstrated that chromothripsis rearrangements may result from chromosome shattering by multiple DSBs, a process which appears distinct from MMBIR as described for other CCRs (Chen et al., 2011; Liu et al., 2011; Liu et al., 2012). Chromosome shattering and nonhomologous repair may be a common mechanism underlying chromothripsis rearrangements associated with developmental malformations.

EXPERIMENTAL PROCEDURES

Patient Material

We obtained informed consent for the genetic analysis of familial DNA from each patient's parents. The genetic analysis was performed according to the

guidelines of the Medical Ethics Committee of the University Medical Center Utrecht. See also Extended Experimental Procedures.

Preparation of Mate-Pair Libraries and SOLiD Sequencing

Mate-paired libraries were prepared and sequenced as described previously (Kloosterman et al., 2011a, 2011b). See also Extended Experimental Procedures.

Bioinformatic Analysis of Mate-Pair Reads

Bioinformatic analysis of mate-pair reads was performed as described previously (Kloosterman et al., 2011a). All custom developed tools are available upon request from the authors. See also Extended Experimental Procedures.

Depth of Coverage Calculations

Depth of sequence coverage was analyzed by an in-house developed Dynamic Window Approach for CNV detection (DWAC-seq: http://fedor21.hubrecht.eu/dwac-seq). Briefly, BAM files for F3 and R3 tags were merged using samtools and the tag densities of cases (test set) were compared to the tag densities of controls (reference set, e.g., parent or unrelated individual). For targeted depth of coverage calculations we generated a common reference based on the concordant mate-pair tags from Patient1_mother, Patient1_father, Patient10_mother, and Patient10_father. The normalized tag count for predicted deletion intervals in patient genomes was measured relative to the normalized tag count for the same intervals in the common reference data set.

Capillary Sequencing of Breakpoints and Analysis of Sequence Reads

Primers for sequencing the breakpoint junctions of structural variants were designed using primer3 software. Where possible, we avoided repetitive elements and designed the primers according to the orientations that were indicated by the mate-pair tags. PCR was performed using Taq polymerase (Invitrogen) with an elongation times of 1–2 min. PCR products were purified from gel when needed. Sanger sequencing reads were aligned to the human reference genome (GRCh37/hg19) using BLAST and BLAT software (http://www.ensembl.org). Hits were analyzed manually to define the exact breakpoint and breakpoint characteristics. PCR breakpoint assays were also used to distinguish de novo junctions from inherited junctions.

qPCR Analysis of Copy Number Changes

For two deletions (18,231 bp and 6,041 bp) in patient 1 we designed primers for qPCR analysis according to the Applied Biosystems HT7900 Real-Time PCR system manual. We performed qPCR reactions using Sybr Green PCR master mix (Applied Biosystems). For normalization, we used primers for GDF7 and PRKD3. Ct values were normalized relative to Ct values for these two control genes and relative to the Ct values of the father. We plotted $2^{\wedge}(-\Delta\Delta Ct)$ values to display relative copy number changes. All reactions were performed in triplicate.

SNP-Array Analysis

SNP-array analysis was performed using Infinium HumanHap300, HumanCNV370-QuadV3 and HumanHap300v1 Genotyping BeadChips (Illumina, Inc., San Diego, CA) and used according to the protocol of the manufacturer.

Data Visualization

Mate-pair and array data were visualized using Circos software and custom R scripts (Krzywinski et al., 2009). We used the chr1, s1, e1, chr2, s2, e2, and orientation(count) values from Table S3 for the colored links in the circos plots. For orientation HH (or hh), we used chr1, s1, chr2, and s2 coordinates; for orientation TT (or tt), we used chr1, e1, chr2, and e2 coordinates; for orientation TH (or th), we used chr1, e1, chr2, and s2 coordinates; for orientation HT (or ht), we used chr1, s1, chr2, and e2 coordinates.

Simulation of Random Breakpoints on Chromosomes 2 and 9

We simulated thousand sets of random double-stranded breaks for chromosomes 2 and 9. For chromosome 2, we used 16 random breaks per set, and for chromosome 9 we used 12 random breaks per set. The average length of the chromosomal fragments resulting from the simulated breaks was calculated for each of the simulated sets. The first and last chromosomal fragments (from the chromosome start to the first break and from the last break to the chromosome end) were not included in the calculations.

ACCESSION NUMBERS

The ENA SRA accession number for the next-generation mate-pair sequencing is ERP001035. The NCBI GEO accession number for the Illumina SNP array data is GSE37906.

SUPPLEMENTAL INFORMATION

Supplemental Information includes Extended Experimental Procedures, three figures, and five tables and can be found with this article online at doi:10.1016/j.celrep.2012.05.009.

LICENSING INFORMATION

ACKNOWLEDGMENTS

We thank the patients and their parents for participation in this study. We thank Gijs van Haaften for critically reading the manuscript. The study was made possible by primary funding of the Department of Medical Genetics of the University Medical Center Utrecht to E.C.

Received: October 7, 2011
Revised: February 9, 2012
Accepted: May 14, 2012
Published online: June 14, 2012

REFERENCES

Astbury, C., Christ, L.A., Aughton, D.J., Cassidy, S.B., Fujimoto, A., Pletcher, B.A., Schafer, I.A., and Schwartz, S. (2004). Delineation of complex chromosomal rearrangements: evidence for increased complexity. Hum. Genet. *114*, 448–457.

Ballarati, L., Recalcati, M.P., Bedeschi, M.F., Lalatta, F., Valtorta, C., Bellini, M., Finelli, P., Larizza, L., and Giardino, D. (2009). Cytogenetic, FISH and array-CGH characterization of a complex chromosomal rearrangement carried by a mentally and language impaired patient. Eur. J. Med. Genet. *52*, 218–223.

Borg, K., Stankiewicz, P., Bocian, E., Kruczek, A., Obersztyn, E., Lupski, J.R., and Mazurczak, T. (2005). Molecular analysis of a constitutional complex genome rearrangement with 11 breakpoints involving chromosomes 3, 11, 12, and 21 and a approximately 0.5-Mb submicroscopic deletion in a patient with mild mental retardation. Hum. Genet. *118*, 267–275.

Chen, J.-M., Férec, C., and Cooper, D.N. (2011). Transient hypermutability, chromothripsis and replication-based mechanisms in the generation of concurrent clustered mutations. Mutat. Res. *750*, 52–59.

Chiang, C., Jacobsen, J.C., Ernst, C., Hanscom, C., Heilbut, A., Blumenthal, I., Mills, R.E., Kirby, A., Lindgren, A.M., Rudiger, S.R., et al. (2012). Complex reorganization and predominant non-homologous repair following chromosomal breakage in karyotypically balanced germline rearrangements and transgenic integration. Nat. Genet. *44*, 390–397, S1.

Crasta, K., Ganem, N.J., Dagher, R., Lantermann, A.B., Ivanova, E.V., Pan, Y., Nezi, L., Protopopov, A., Chowdhury, D., and Pellman, D. (2012). DNA breaks and chromosome pulverization from errors in mitosis. Nature *482*, 53–58.

De Gregori, M., Ciccone, R., Magini, P., Pramparo, T., Gimelli, S., Messa, J., Novara, F., Vetro, A., Rossi, E., Maraschio, P., et al. (2007). Cryptic deletions

are a common finding in ''balanced'' reciprocal and complex chromosome rearrangements: a study of 59 patients. J. Med. Genet. *44*, 750–762.

de Pater, J.M., Ippel, P.F., van Dam, W.M., Loneus, W.H., and Engelen, J.J.M. (2002). Characterization of partial trisomy 9p due to insertional translocation by chromosomal (micro)FISH. Clin. Genet. *62*, 482–487.

Feenstra, I., Hanemaaijer, N., Sikkema-Raddatz, B., Yntema, H., Dijkhuizen, T., Lugtenberg, D., Verheij, J., Green, A., Hordijk, R., Reardon, W., et al. (2011). Balanced into array: genome-wide array analysis in 54 patients with an apparently balanced de novo chromosome rearrangement and a meta-analysis. Eur. J. Hum. Genet. *19*, 1152–1160.

Gajecka, M., Gentles, A.J., Tsai, A., Chitayat, D., Mackay, K.L., Glotzbach, C.D., Lieber, M.R., and Shaffer, L.G. (2008). Unexpected complexity at breakpoint junctions in phenotypically normal individuals and mechanisms involved in generating balanced translocations t(1;22)(p36;q13). Genome Res. *18*, 1733–1742.

Giardino, D., Corti, C., Ballarati, L., Finelli, P., Valtorta, C., Botta, G., Giudici, M., Grosso, E., and Larizza, L. (2006). Prenatal diagnosis of a de novo complex chromosome rearrangement (CCR) mediated by six breakpoints, and a review of 20 prenatally ascertained CCRs. Prenat. Diagn. *26*, 565–570.

Granot-Hershkovitz, E., Raas-Rothschild, A., Frumkin, A., Granot, D., Silverstein, S., and Abeliovich, D. (2011). Complex chromosomal rearrangement in a girl with psychomotor-retardation and a de novo inversion: inv(2)(p15;q24.2). Am. J. Med. Genet. A. *155A*, 1825–1832.

Gribble, S.M., Prigmore, E., Burford, D.C., Porter, K.M., Ng, B.L., Douglas, E.J., Fiegler, H., Carr, P., Kalaitzopoulos, D., Clegg, S., et al. (2005). The complex nature of constitutional de novo apparently balanced translocations in patients presenting with abnormal phenotypes. J. Med. Genet. *42*, 8–16.

Hastings, P.J., Ira, G., and Lupski, J.R. (2009a). A microhomology-mediated break-induced replication model for the origin of human copy number variation. PLoS Genet. *5*, e1000327.

Hastings, P.J., Lupski, J.R., Rosenberg, S.M., and Ira, G. (2009b). Mechanisms of change in gene copy number. Nat. Rev. Genet. *10*, 551–564.

Hehir-Kwa, J.Y., Rodríguez-Santiago, B., Vissers, L.E., de Leeuw, N., Pfundt, R., Buitelaar, J.K., Pérez-Jurado, L.A., and Veltman, J.A. (2011). De novo copy number variants associated with intellectual disability have a paternal origin and age bias. J. Med. Genet. *48*, 776–778.

Houge, G., Liehr, T., Schoumans, J., Ness, G.O., Solland, K., Starke, H., Claussen, U., Strømme, P., Akre, B., and Vermeulen, S. (2003). Ten years follow up of a boy with a complex chromosomal rearrangement: going from a > 5 to 15-breakpoint CCR. Am. J. Med. Genet. A. *118A*, 235–240.

Kloosterman, W.P., Guryev, V., van Roosmalen, M., Duran, K.J., de Bruijn, E., Bakker, S.C.M., Letteboer, T., van Nesselrooij, B., Hochstenbach, R., Poot, M., and Cuppen, E. (2011a). Chromothripsis as a mechanism driving complex de novo structural rearrangements in the germline. Hum. Mol. Genet. *20*, 1916–1924.

Kloosterman, W.P., Hoogstraat, M., Paling, O., Tavakoli-Yaraki, M., Renkens, I., Vermaat, J.S., van Roosmalen, M.J., van Lieshout, S., Nijman, I.J., Roessingh, W., et al. (2011b). Chromothripsis is a common mechanism driving genomic rearrangements in primary and metastatic colorectal cancer. Genome Biol. *12*, R103.

Krzywinski, M., Schein, J., Birol, I., Connors, J., Gascoyne, R., Horsman, D., Jones, S.J., and Marra, M.A. (2009). Circos: an information aesthetic for comparative genomics. Genome Res. *19*, 1639–1645.

Lieber, M.R. (2008). The mechanism of human nonhomologous DNA end joining. J. Biol. Chem. *283*, 1–5.

Lieber, M.R. (2010). The mechanism of double-strand DNA break repair by the nonhomologous DNA end-joining pathway. Annu. Rev. Biochem. *79*, 181–211.

Liu, P., Erez, A., Nagamani, S.C.S., Dhar, S.U., Kołodziejska, K.E., Dharmadhikari, A.V., Cooper, M.L., Wiszniewska, J., Zhang, F., Withers, M.A., et al. (2011). Chromosome catastrophes involve replication mechanisms generating complex genomic rearrangements. Cell *146*, 889–903.

Liu, P., Carvalho, C.M., Hastings, P., and Lupski, J.R. (2012). Mechanisms for recurrent and complex human genomic rearrangements. Curr. Opin. Genet. Dev. *22*, 1–10.

Magrangeas, F., Avet-Loiseau, H., Munshi, N.C., and Minvielle, S. (2011). Chromothripsis identifies a rare and aggressive entity among newly diagnosed multiple myeloma patients. Blood *118*, 675–678.

Maher, C.A., and Wilson, R.K. (2012). Chromothripsis and human disease: piecing together the shattering process. Cell *148*, 29–32.

McVey, M., and Lee, S.E. (2008). MMEJ repair of double-strand breaks (director's cut): deleted sequences and alternative endings. Trends Genet. *24*, 529–538.

Medvedev, P., Stanciu, M., and Brudno, M. (2009). Computational methods for discovering structural variation with next-generation sequencing. Nat. Methods *6*(11, Suppl), S13–S20.

Molenaar, J.J., Koster, J., Zwijnenburg, D.A., van Sluis, P., Valentijn, L.J., van der Ploeg, I., Hamdi, M., van Nes, J., Westerman, B.A., van Arkel, J., et al. (2012). Sequencing of neuroblastoma identifies chromothripsis and defects in neuritogenesis genes. Nature *483*, 589–593.

Pellestor, F., Anahory, T., Lefort, G., Puechberty, J., Liehr, T., Hédon, B., and Sarda, P. (2011). Complex chromosomal rearrangements: origin and meiotic behavior. Hum. Reprod. Update *17*, 476–494.

Poot, M., van't Slot, R., Leupert, R., Beyer, V., Passarge, E., and Haaf, T. (2009). Three de novo losses and one insertion within a pericentric inversion of chromosome 6 in a patient with complete absence of expressive speech and reduced pain perception. Eur. J. Med. Genet. *52*, 27–30.

Rausch, T., Jones, D.T.W., Zapatka, M., Stütz, A.M., Zichner, T., Weischenfeldt, J., Jäger, N., Remke, M., Shih, D., Northcott, P.A., et al. (2012). Genome sequencing of pediatric medulloblastoma links catastrophic DNA rearrangements with TP53 mutations. Cell *148*, 59–71.

Schluth-Bolard, C., Delobel, B., Sanlaville, D., Boute, O., Cuisset, J.-M., Sukno, S., Labalme, A., Duban-Bedu, B., Plessis, G., Jaillard, S., et al. (2009). Cryptic genomic imbalances in de novo and inherited apparently balanced chromosomal rearrangements: array CGH study of 47 unrelated cases. Eur. J. Med. Genet. *52*, 291–296.

Simsek, D., and Jasin, M. (2010). Alternative end-joining is suppressed by the canonical NHEJ component Xrcc4-ligase IV during chromosomal translocation formation. Nat. Struct. Mol. Biol. *17*, 410–416.

Stephens, P.J., Greenman, C.D., Fu, B., Yang, F., Bignell, G.R., Mudie, L.J., Pleasance, E.D., Lau, K.W., Beare, D., Stebbings, L.A., et al. (2011). Massive genomic rearrangement acquired in a single catastrophic event during cancer development. Cell *144*, 27–40.